X-RAY AMORPHOUS PHASES IN TERRESTRIAL ANALOG VOLCANIC SEDIMENTS: IMPLICATIONS FOR AMORPHOUS PHASES IN GALE CRATER, MARS. R. J. Smith[1], B. Horgan[1], E. Rampe[2], E. Dehouck[3], and R. V. Morris[2], [1]Purdue University (rebeccajsmith@purdue.edu), [2]Johnson Space Center, [3]Institut de Recherche en Astrophysique et Planétologie, UPS/CNRS/OMP.

Introduction: X-ray diffraction (XRD) amorphous phases have been found as major components (~15-60 wt%) of all rock and soil samples measured by the CheMin XRD instrument in Gale Crater, Mars [1-4]. The nature of these phases is not well understood and could be any combination of primary (e.g., glass) and secondary (e.g., allophane) phases. Amorphous phases form in abundance during surface weathering on Earth [e.g., 5-7]. Yet, these materials are poorly characterized, and it is not certain how properties like composition and structure change with formation environment.

The presence of poorly crystalline phases can be inferred from XRD patterns by the appearance of a low angle rise (<~10° 2θ) or broad peaks in the background at low to moderate 2θ angles (amorphous humps) [8-9]. CheMin mineral abundances combined with bulk chemical composition measurements from the Alpha Particle X-ray Spectrometer (APXS) have been used to estimate the abundance and composition of the XRD amorphous materials in soil and rock samples on Mars [2-4, 10]. Here we apply a similar approach to a diverse suite of terrestrial samples – modern soils, glacial sediments, and paleosols – in order to determine how formation environment, climate, and diagenesis affect the abundance and composition of X-ray amorphous phases.

Methods: We apply the mass balance calculations like [10] to a suite of terrestrial samples:

$$y_{cryst} = \Sigma_i(y_i)(x_i); \text{ with } \Sigma_i x_i = 100$$

$$y_{amorph} = \frac{y_{bulk} - y_{cryst}}{x_{amorph}} + y_{cryst}$$

where $y_{\square}$ represents the abundance of a given oxide in a given mineral (y_i), the bulk sample (y_{bulk}), the crystalline component (y_{crst}), or the amorphous component (y_{amorph}); x_i represents the amorphous-free abundances of crystalline phases; and x_{amorph} is the proportion of amorphous component. Mineral abundances are derived from Rietveld refinements using JADE software of XRD patterns measured on a Panalytical instrument with a Co source. Initial measurements were performed without an internal standard in order to be more relevant to CheMin measurements. Elemental chemistry is measured via XRF, titration (FeO), IR (SO_3), and INAA (Cl).

The abundances of X-ray amorphous materials can be calculated in two ways: (1) Modeled in the Rietveld refinement of the XRD data. This method is strongly dependent on the modeled background and on the assigned reference intensity ratio (RIR) of the amorphous material [8-9]. The amorphous phase abundances in Figure 1 are derived from a background modeled automatically in the refinement and an RIR similar to amorphous silica. (2) The abundances of amorphous phases can also be adjusted in the mass balance calculations in order to find the lowest percentage of amorphous material needed to ensure non-negative wt. % oxide solutions for the amorphous phases [10]. Thus, this method finds only the lower limit for the abundance of amorphous material present.

Our sample suite includes sediments from recently exposed glaciated volcanoes in Three Sisters, OR (<1 mm size fraction), modern Hawaiian volcanic soils ranging in age and climate, and volcanic paleosols from Oregon that formed in different climates and underwent varying burial and diagenesis processes. All analyses were done on powdered samples (<10 μm).

Results: Preliminary analysis of two samples has been completed to date, as shown in Figure 1. The glacial moraine sediments display the smallest "amorphous humps" (Figure 1a), and are modeled with the

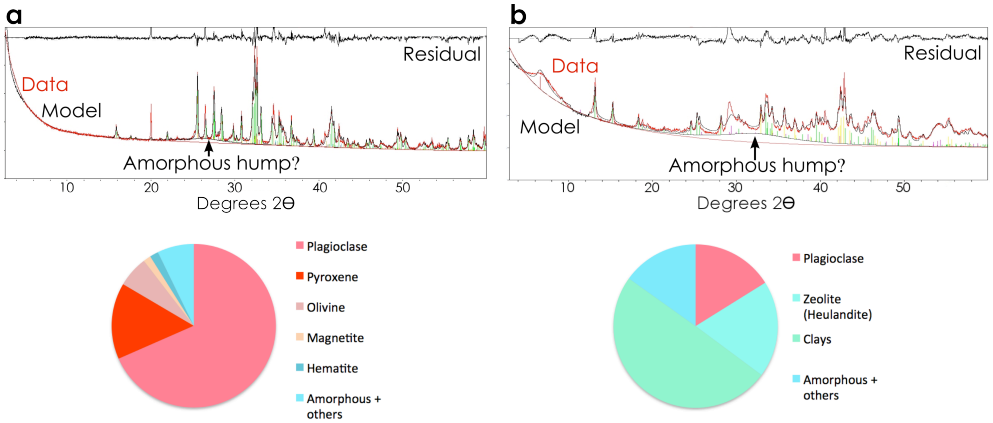

Figure 1. XRD patterns with Rietveld refinement models (top) and derived phase abundances (bottom) for two samples. (a) 160814X: Glacial sediment from a lateral moraine (amorphous phases ~7%). (b) TC-6: Well-drained paleosol sample formed in an arid climate (amorphous phases ~21%).

lowest abundance of amorphous components (~7%) and the highest abundance of primary minerals, suggesting that these samples are minimally altered. Yet, the amorphous hump for the glacial sample in Figure 1a is narrower and at slightly lower angle (~27° 2θ) than that of basaltic glass (~30° 2θ, [9]). Thus, the amorphous component of this sample is not consistent with basaltic glass. Preliminary mass balance calculations require ~21% amorphous component and indicate that the amorphous component is depleted in Al_2O_3 and FeO, and elevated in SiO_2, TiO_2, Fe_2O_3, MnO, K_2O, P_2O_5, and Cl relative to the crystalline components (Table 1). FeO is the oxide that limits the minimum abundance of an amorphous component.

All paleosol samples are mixtures of primary (plagioclase), pedogenic (phyllosilicates), and diagenetic (zeolites and possibly phyllosilicates) phases. Figure 1b displays a highly elevated background, an amorphous hump near 33° 2θ, and is modeled with ~21% amorphous phases. Preliminary mass balance calculations require ~76% amorphous component and indicate that the amorphous component is depleted in Al_2O_3, and elevated in SiO_2, TiO_2, FeO, Fe_2O_3, MnO, P_2O_5, and Cl relative to the crystalline components (Table 1). K_2O is the oxide that limits the minimum abundance of an amorphous component.

While we do not expect either of these samples to be exact process analogs for the lacustrine Cumberland sample from Gale Crater, Mars, there are some similarities. As with our terrestrial samples, the amorphous component of Cumberland is depleted in Al_2O_3 and elevated in TiO_2, MnO, P_2O_5, and Cl relative to the crystalline component (Table 1). However, the terrestrial samples have much more SiO_2 in their amorphous components than Cumberland.

Discussion: The two samples studied thus far differ in mineralogy and in amorphous component abundances and compositions, and we expect similar variability among the rest of the sample suite. These differences could result from chemistry of alteration fluids, climate, weathering time or rate, and/or diagenetic history. It is notable that XRD appears to consistently underestimate the abundance of amorphous phases relative to mass balance. This could be due to an incorrect RIR for the amorphous phases, which is realistic given the evidence for diversity in amorphous composition between samples. For the paleosol sample, this could also be exacerbated by a poor constraint on the composition of the clay mineral– a slightly different chemical formula for illite reduces the mass-balance derived abundance to ~64%. MSL is equipped with an Evolved Gas Analaysis (EGA) instrument, and clay mineral compositions are more readily identified. Further analysis of this sample suite (QXRD, EGA, TEM, spectra, grain size experiments) will help determine the limitations of the mass-balance technique and identify the amorphous phase(s) present.

References: [1] Bish et al. (2013) *Science, 341*. [2] Blake et al. (2013) *Science, 341*. [3] Vaniman et al. (2014) *Science, 343*. [4] Morris et al. (2016) *PNAS, 113*, 7071-7076. [5] Colman (1982) *Geo. Survey Prof. Paper 1246*. [6] Wada (1987) *Chem. Geo., 60*, 17-28. [7] Fedotov et al. (2006) *Eur. Soil Sci., 39*, 738-747. [8] Rampe et al. (2013) *LPSC XLIV*, #1188. [9] Achilles et al. (2013) *LPSC XLIV,* #3072. [10] Dehouck et al. (2014) *JGR*, *119,* 2640-2657. [11] Retallack et al. (1999) *Geo. Soc. Am., 344*.

Oxides (wt.%)	Glacial Moraine 160814X			Oxidized Paleosol TC-6			Cumberland, Mars [10]		
	Bulk	Crystalline Component	Amorphous (21.5%)[a]	Bulk	Crystalline Component	Amorphous (76%)[a]	Bulk	Crystalline Component	Amorphous (30%)[b]
SiO_2	53.78	52.37	60.01	53.87	47.51	65.89	43.02	46.0	36.1
TiO_2	1.36	0.01	6.31	0.9	0.00	1.34	0.97	0.4	2.3
Al_2O_3	17.33	20.55	5.94	13.02	40.10	7.38	8.57	11.5	1.8
Cr_2O_3	0.01	0.00	0.05	0.01	0.00	0.01	0.43	0.0	1.4
FeO	5.5	7.02	**0.06**	0.6	0.00	0.89	22.35	21.3[c]	24.7[c]
Fe_2O_3	4.3	3.15	8.58	6.73	0.00	10.00	-	-	-
MnO	0.145	0.00	0.68	0.146	0.00	0.22	0.27	0.0	0.8
MgO	4.36	4.88	2.56	2.34	0.00	3.48	9.41	9.7	8.8
CaO	7.54	7.56	7.62	4.57	4.43	5.47	6.29	6.0	6.9
Na_2O	3.99	4.46	2.36	2.58	1.13	3.50	2.98	2.2	4.8
K_2O	0.93	0.00	4.34	1.42	6.83	**0.07**	0.50	0.4	0.7
P_2O_5	0.26	0.00	1.21	0.09	0.00	0.13	0.95	0.0	3.2
SO_3	0.01	0.00	0.05	0.03	0.00	0.04	2.57	2.7	2.2
Cl	0.05	0.00	0.23	1.06	0.00	1.58	1.39	0.2	4.2
Total	99.57	100	100	87.37	100	100	99.70	100.4	97.9

Table 1. Calculated wt. % oxides for crystalline and XRD amorphous components in the two patterns shown in Figure 1 compared to Rocknest soil sample from Mars. [a]X-ray amorphous phase abundance derived from abundance needed to ensure non-negative wt. % oxide abundances for amorphous component. Values in bold indicate the oxide enforcing this lower limit. [b] "Best-case" calculations from a Rietveld refinement with 30% amorphous phases with a Griffith saponite composition [10].